Received: 10 November 2014 ■ Revised: 18 March 2015 ■ Accepted: 20 March 2015 ■ Publication: 31 March 2015

JNIRS JOURNAL OF NEAR INFRARED SPECTROSCOPY

Decoding answers to four-choice questions using functional near infrared spectroscopy

Noman Naseer[a] and Keum-Shik Hong[a*,b]

[a]Department of Cogno-Mechatronics Engineering, Pusan National University, 2 Busandaehak-ro, Geumjeong-gu, Busan 609-735, Korea

[b]School of Mechanical Engineering, Pusan National University, 2 Busandaehak-ro, Geumjeong-gu, Busan 609-735, Korea.
E-mail: kshong@pusan.ac.kr

This paper presents a functional near infrared (NIR) spectroscopy-based paradigm that can be used to decode answers to four-choice questions. Ten healthy subjects were asked to perform one of the four different brain activities, that is, right-hand motor imagery (RMI), left-hand motor imagery (LMI), mental arithmetic (MA) and mental counting (MC), to answer the given four-choice questions. In selecting the A, B, C or D choices, the subjects were asked to perform RMI, LMI, MA or MC, respectively. Signals from the primary motor and prefrontal cortices were acquired simultaneously using a continuous-wave functional NIR spectroscopy system. The four activities were classified using multiclass linear discriminant analysis to decode the answers to an average accuracy of 73.3% across the 10 subjects. The results demonstrate the potential of functional NIR spectroscopy to decode answers to four-choice questions using four different intentionally generated brain activities as control signals.

Keywords: functional near infrared spectroscopy, brain–computer interface, multiple-decision decoding, linear discriminant analysis, classification, neuroimaging

Introduction

Decision decoding is of particular importance in cases of totally locked-in syndrome (LIS), amyotrophic lateral sclerosis (ALS), anarthria and other such severe motor disabilities where patients (despite being fully conscious) cannot communicate naturally.[1] A brain–computer interface (BCI) can, by bypassing the central nervous system, provide a means of communication for such people.[2] Invasive BCIs are capable of controlling a prosthetic device by directly acquiring brain signals from the grey matter:[3] However, non-invasive BCIs usually use brain signals from/on the scalp in making commands to a computer, in which those brain signals are generated from various brain activities. Crucially, for such BCI purposes, brain activities can be generated using the process of thinking alone: no body movement is required.

BCIs have been shown to work well in a significant number of previous studies using a variety of brain-signal acquisition methods including electroencephalography (EEG),[2,4,5] functional magnetic resonance imaging (fMRI)[1,6] and functional near infrared (NIR) spectroscopy.[7–13] Functional NIR spectroscopy is an optical brain-imaging modality that has the advantages of being portable, cheap and relatively simple. Its spatial resolution is comparable with that of EEG. Since Jobsis[14] first introduced the principle of NIR spectroscopy in 1977, it has been applied to the fields of brain mapping, brain-state decoding and BCI.[15–27]

In functional NIR spectroscopy-based BCI applications, the user can communicate by evoking different patterns of activation in a particular brain region. This can be done by performing different mental tasks, such as motor imagery,[7,8,9,12] mental arithmetic (MA),[13,28–31] music imagery[10,28,29] and others.[10] These evoked patterns can be detected and recognised as different activities by classifying them. The relevant command signals can then be produced to communicate with a computer in a manner premeditated by the user.

ISSN: 0967-0335
doi: 10.1255/jnirs.1145

The feasibility of using motor imagery for the purpose of BCI has been established in previous functional NIR spectroscopy and EEG studies.[4,7–9,12,32–34] Using motor imagery is advantageous from the neurorehabilitation perspective, as the brain area activated by it is similar to that activated by motor execution. For the same reason, it is also considered to be an unavoidable way to provide BCI control for paralysed people. However, a disadvantage of motor imagery is the fact that it might be difficult to perform it for some people with congenital and/or longstanding motor disabilities because of cortical reorganisation.[35,36] Other than motor imagery, activities such as mental arithmetic (MA) and mental counting (MC) (when targeting the prefrontal cortex) are also good choices for BCI application,[29,31,37] particularly because the prefrontal cortex usually is not implicated in motor disabilities. The use of prefrontal cortex activities for BCI purposes also is advantageous because noise owing to hair artefacts is less severe. Since hair and hair follicles are strong absorbers of light in the NIR region, hair-free regions provide improved signal strength and penetration depth.[38] Some NIR spectroscopy-BCI studies have shown promising results in using the prefrontal mental-arithmetic and mental-counting activities.[29] A disadvantage, however, is that both sweat and muscle twitches can affect prefrontal-cortex-originated NIR spectroscopy signals.

EEG- and NIR-based BCIs have been shown to work well for binary decoding and yes/no communication.[13,39–41] However, they have not yet been tested for multiple-decision-based communication, whereas fMRI-based BCI has shown to be feasible for multiple-decision decoding.[1] However, fMRI equipment is not portable, which reflects the fact that it is unsuitable for daily-life usage.

In the present study, we decoded answers to four-choice questions based on four different brain activities acquired using concurrent fNIRS measurement from the primary motor and prefrontal cortices. The four activities utilised were MA, mental counting (MC), right-hand motor imagery (RMI) and left-hand motor imagery (LMI). After being acquired, the signals were preprocessed and classified using multiclass linear discriminant analysis (LDA) to decode the answers. The overall decoding accuracy across 10 subjects was 73.3%. To the best of our knowledge, this is the first functional NIR spectroscopy-based work to decode responses in a four-choice question paradigm using four different intentionally generated cognitive tasks acquired simultaneously from the primary motor and prefrontal cortices.

Materials and methods

Signal acquisition

Functional NIR spectroscopy uses near infrared-range (650~1000 nm) emitters to propagate light (through photon scattering) several centimetres through the scalp, skull and tissues to the microvessels in the cortex, where brain haemodynamics are functionally imaged.[42] In the brain, the photons are absorbed, primarily by oxygenated and deoxygenated haemoglobins (HbO and HbR), or undergo multiple scattering in returning to the surface of the head. There, suitably positioned detectors record the returning photons. The changes in the concentrations of HbO and HbR can then be determined using the modified Beer–Lambert law,[43] and by monitoring those changes, conclusions as to brain-functional activity can be drawn. In this study, we used a multichannel continuous-wave imaging system, DYNOT (dynamic near infrared optical tomography; NIRx Medical Technologies, NY), to acquire NIR signals at a sampling rate of 1.81 Hz for two wavelengths λ_1 = 760 nm and λ_2 = 830 nm. The selection of the sampling rate is in accordance with the literature.[11–13,23]

Subjects

Ten healthy subjects (all right-handed, male, mean age 28.2 ± 6.6) participated in the experiment. The reason for recruiting only right-handed subjects was to minimize any variations in the haemodynamic response owing to differences caused by hemispheric dominance. None of the subjects had a history of any psychiatric or neurological disorder. All of them had normal or corrected-to-normal vision. They provided their verbal informed consent after the experimental procedure was explained to them in detail. The experiment was conducted in accordance with the latest Declaration of Helsinki.

Optode configuration and positioning

The positioning of optodes in the NIR experiment is of vital importance to ensure that the photons travel through the area activated by brain activity. Usually, the international 10–20 system has been used as a basis for optode positioning.[44] The distance between an emitter and a detector also is very important, as it affects the penetration depth and signal strength. The midpoint between the emitter and the detector is considered as a point of maximum penetration depth. An increase in the emitter-detector distance, for example, corresponds to an increase in the imaging depth,[45] whereas a separation of more than 5 cm might result in weak and unusable signals.[46] To measure haemodynamic response signals from the cortical area, usually an emitter–detector separation of 3–4 cm is applied.[47]

In consideration of the above points, six NIR light emitters and six detectors (with a 3 cm interoptode distance) were positioned over the primary motor cortex in both hemispheres to measure the signals from RMI and LMI; see Figure 1(a). The primary motor cortex area is well known as an area of the brain activated by motor imagery.[48,49] The 12 optodes were arranged in such a way as to make 17 channels in each hemisphere. Additionally, nine channels were made by positioning three emitters and five detectors over the prefrontal cortex, with an interoptode distance of 3 cm, to measure the signals from MA and MC; see Figure 1(b). The total numbers of optodes and channels, respectively, are 32 (24 over the primary motor cortex and eight over the prefrontal cortex) and 43 (17 × 2 over the primary motor cortex and nine over the prefrontal cortex).

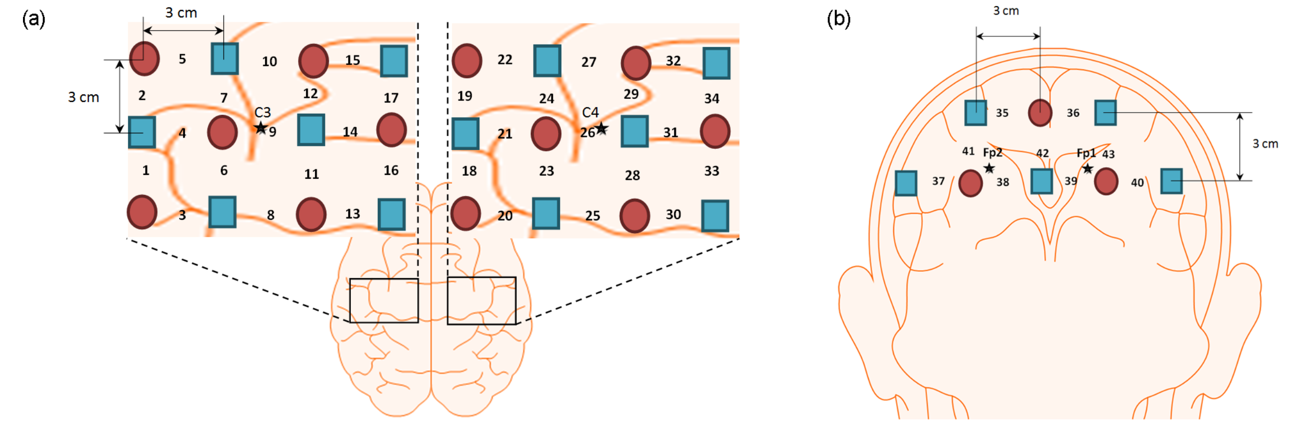

Figure 1. Optode positioning and channel configuration (red circles represent emitters, blue squares represent detectors). In (a), six emitters and six detectors (over each hemisphere) were used to acquire signals corresponding to right- and left-hand motor imageries. In (b), three emitters and five detectors were used to acquire signals corresponding to mental arithmetic and mental counting. The optode positioning has been made with reference to Fp1 and Fp2 of the International 10–20 System.

Experimental procedure

In preparation for the experiments, the subjects were asked to relax for 5 min in order to remove any prior existing haemodynamic response activations owing to previous activities. They were also advised not to drink coffee or alcohol or smoke cigarettes at least 3 h before the experiment. Each subject was seated in a comfortable chair facing a 15.6 inch monitor located at a distance of approximately 65~70 cm in a dimly lighted room. They were asked to remain relaxed and to restrict their body movements or thoughts during the experiments. Each experiment started with a 60 s rest period to setup a baseline value, followed by the following sequence: (1) 20 s rest period, (2) 10 s question presentation period, (3) 10 s decision period (see Figure 2). This 40 s sequence was repeated 40 times. The total duration of the experiment for each subject, therefore, was 1600 s. The task period of 10 s was chosen in accordance with the literature.[9,10,12,28] It has been shown that a 10~12 s task is sufficient to adequately acquire the haemodynamic signals corresponding to brain activities.[9,10] During the question-presentation period in each repetition, a four-choice question was presented on the screen for 10 s. The total number of questions presented, and thereby the trials per subject, then, was 40. Since 40 trials is a small number to accept the results statistically and to estimate a meaningful model, four such experimental sessions were performed by each subject. The final number of trials per subject was therefore 160. The subjects were asked to make a decision on the four-choice question appearing on the screen during each decision period. To answer the questions in choices A, B, C or D, the subjects were required to perform RMI, LMI, MA or MC, respectively. The instruction to select the specific option to perform the specific task was displayed on the screen during the question presentation period. For the RMI and LMI tasks, the subjects were asked to kinesthetically image

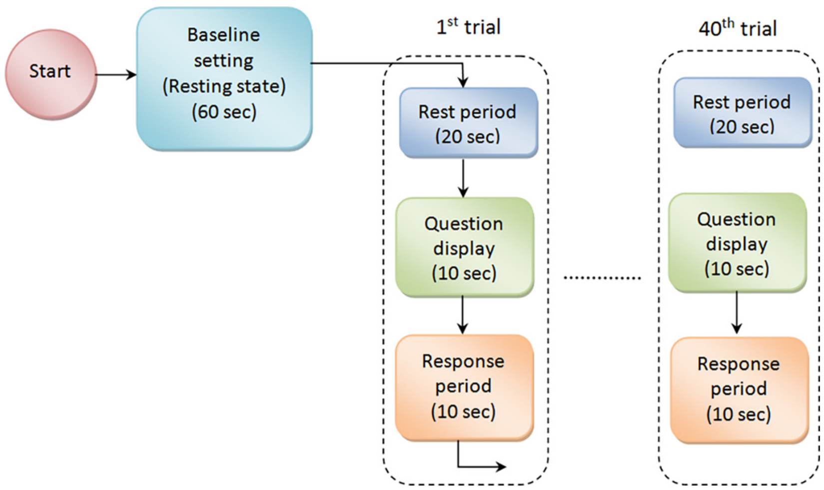

Figure 2. Experimental paradigm: After the initial rest period of 60 s to set up the baseline values, the 20–10–10 s sequences corresponding to rest, question-display and response periods, respectively, were repeated 40 times for each subject in one experimental session.

the squeezing of a rubber ball with their right and left hands, respectively, while avoiding any muscular tension, as in Coyle *et al.*[8] For the MA task, the subjects were asked to mentally perform a series of arithmetic calculations appearing on the screen in a pseudorandom order. These calculations consisted of subtraction of a two-digit number (between 10 and 20) from a three-digit number throughout the 10 s task period, with successive subtraction of a two-digit number from the result of the previous subtraction (e.g. 730 – 17, 713 – 12, 701 – 15, etc.).[13,29] The MC required the subjects to count backward starting from any three-digit number of their choice. For all of the tasks, the subjects were asked to maintain the corresponding cognitive activity throughout the 10 s decision period. To make the subjects familiar with the experiment, a practice session was performed prior to the actual experiments.

Signal processing

The raw light-intensity signals were first used to calculate the concentration changes of HbO and HbR ($\Delta c_{HbO}(t)$ and $\Delta c_{HbR}(t)$, together $\Delta c_{HbX}(t)$), where HbX ∈ {HbO, HbR}, according to the modified Beer–Lambert law:

$$\begin{pmatrix}\Delta c_{HbO}(t)\\ \Delta c_{HbR}(t)\end{pmatrix} = \begin{pmatrix}\alpha_{HbO}(\lambda_1) & \alpha_{HbR}(\lambda_1)\\ \alpha_{HbO}(\lambda_2) & \alpha_{HbR}(\lambda_2)\end{pmatrix}^{-1} \begin{pmatrix}\dfrac{\Delta A(t,\lambda_1)}{d(\lambda_1)}\\ \dfrac{\Delta A(t,\lambda_2)}{d(\lambda_2)}\end{pmatrix} \frac{1}{l} \tag{1}$$

where $\Delta A(t;\lambda_j)$ (j = 1,2) is the unit-less absorbance (optical density) variation of a light emitter of wavelength λ_j, $a_{HbX}(\lambda j)$ is the extinction coefficient of HbX in $\mu M^{-1} mm^{-1}$, d is the unit-less differential pathlength factor (DPF) and l is the emitter/detector distance (in millimeters). NIRS-SPM[50] was used to apply the modified Beer–Lambert law. The default values of 7.15, 5, 1.48 $\mu M^{-1} mm^{-1}$, 3.84 $\mu M^{-1} mm^{-1}$, 2.23 $\mu M^{-1} mm^{-1}$ and 1.79 $\mu M^{-1} mm^{-1}$ for $d(\lambda_1)$, $d(\lambda_2)$, $a_{HbO}(\lambda_1)$, $a_{HbO}(\lambda_2)$, $a_{HbR}(\lambda_1)$ and $a_{HbR}(\lambda_2)$ respectively, were used.

The $\Delta C_{HbX}(t)$ signals were then normalised by dividing them by the mean value during the 60 s baseline/rest period. The $\Delta C_{HbX}(t)$ signals obtained contain several physiological noises.[51,52] In order to remove the high-frequency physiological noises owing to heartbeat and respiration, the signals were low-pass filtered using a fourth-order Butterworth filter set to a cutoff frequency of 0.3 Hz. The signals were also high-pass filtered with a cutoff frequency of 0.1 Hz to minimize the effect of low-frequency oscillations such as Mayer waves.

Feature selection and classification

The signal slope (SS) and signal mean (SM) of the $\Delta C_{HbX}(t)$ signals averaged over all of the channels were considered as the features for classification, as they had been shown to work well in the previous studies.[12,53,54] The SS values were determined by linearly fitting a regression line (using the *polyfit* command in Matlab) to all of the data points in a 2~7 s time window during the 10 s decision-making period, while the SM values were acquired by averaging all of the data points in the same 2~7 s time window. The reason for selecting a 2~7 s time window was to improve the classification accuracy.[12,55,56] The resulting feature set consisted of 160 four-dimensional data points for each subject. Prior to classification, all of the features were normalised between 0 and 1 using the equation

$$\boldsymbol{x}' = \frac{\boldsymbol{x} - \min \boldsymbol{x}}{\max \boldsymbol{x} - \min \boldsymbol{x}} \tag{2}$$

where $\boldsymbol{x} \in R^n$ (n = 160 in this paper) denotes the original SM and SS data, $\boldsymbol{x}'$ denotes the rescaled values between 0 and 1, max $\boldsymbol{x}$ is the largest value, and min x is the smallest value. In this research, we used multiclass LDA to classify the features derived from the four different activities. LDA is a widely used linear classifier offering the advantages of simplicity and computational speed.[57] For additional details on multiclass LDA, see Li *et al.*[58] Finally, the classification results were evaluated using leave-one-subject-out cross-validation. This uses the features of one subject for testing and the features of the remaining subjects for training. The process was repeated until all the subjects' features had been tested.

Results

The all-subject-averaged decoding accuracy was 73.3%. The individual-subject decoding accuracies, given in Table 1, were well above the chance level. It should be noted that the chance level in our paradigm was 25%. Since the percentages of the four responses were not the same, the accuracies of individual-option decoding were calculated for all subjects (see Figure 3). The all-subject accuracies in decoding A, B, C and D responses were 78.9%, 72.3%, 74.1% and 67.8%, respectively. The higher accuracy in decoding answer A implies that the signals from RMI were more easily distinguished than those from LMI, MA or MC. To see which of the proposed features

Table 1. Overall decoding accuracies of all subjects.

Subjects	Questions asked	Correctly decoded	Decoding accuracy (%)
1	160	109	68.1
2	160	114	71.2
3	160	124	77.5
4	160	116	71.8
5	160	119	72.5
6	160	117	73.1
7	160	126	78.7
8	160	114	71.4
9	160	119	74.3
10	160	115	71.8
Total	1600	1173	73.3

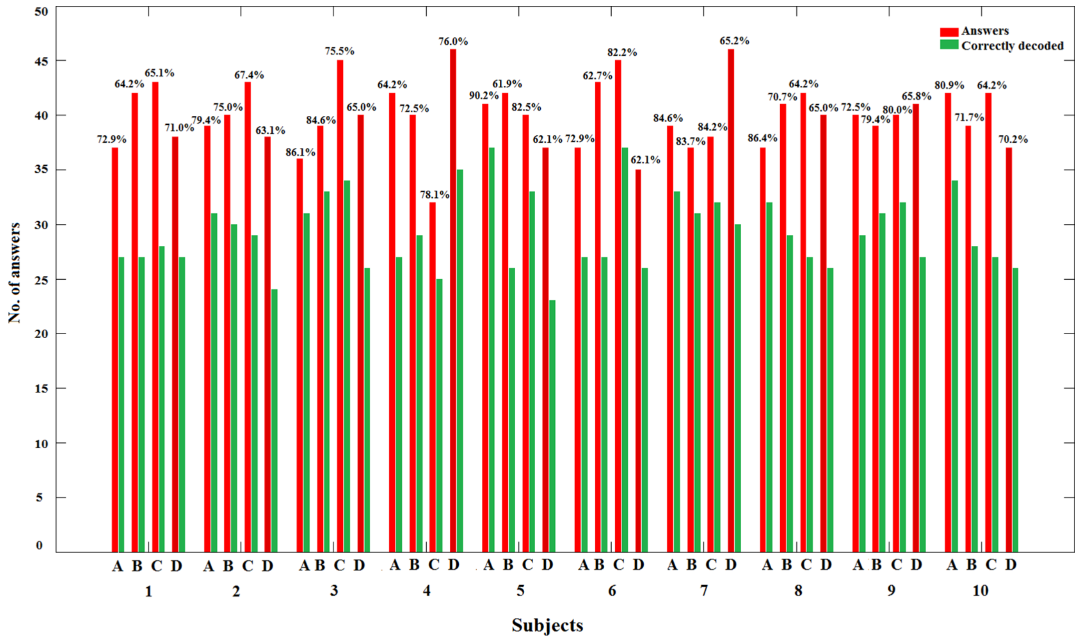

Figure 3. Classification accuracies (correctly decoded/total answers) of four options for all the subjects. Options A, B, C and D for Subject 1 were selected 37, 42, 43 and 48 times, respectively, and were correctly decoded 27, 27, 28 and 27 times, respectively, which indicates that RMI, LMI, MA and MC were correctly classified 72.9%, 64.2%, 65.1% and 71.0%, respectively.

were more discriminative, classification was performed using different combinations of SS and SM of $\Delta c_{HbZ}(t)$. The all-subject-average decoding accuracy using SS of HbO and SM of HbO, SS of HbO and SM of HbR, SS of HbO and SS of HbR, SS of HbR and SM of HbO, SS of HbR and SM of HbR, and SM of HbO and SM of HbR were 70.2%, 66.1%, 65.8%, 62.7%, 61.1% and 63.9%, respectively. The analysis of these results revealed that SM and SS of HbO signals were more discriminative than those of HbR signals. However, the inclusion of SM and SS of HbR, though less discriminative individually, did improve the overall accuracy.

Discussion

This paper presents a method by which four different functional NIR spectroscopy signals can be reliably originated to encode four distinct information units to answer four-choice questions. The answers were successfully decoded to an average accuracy of 73.3% across all the subjects, thus establishing the suitability of decoding answers to four-choice questions using functional NIR spectroscopy. It should be noted that the classification accuracies varied among the subjects and even among the trials. This can be attributed to both individual-subject differences and trial-to-trial variations in the signals caused by background activity or as-yet-unknown sources.[59–62] To the best of our knowledge, this is the first functional NIR spectroscopy study to perform four classifications of four different covert tasks in decoding answers to four-choice questions. Shin and Jeong[63] performed four-class classification of functional NIR spectroscopy signals for BCI; however, their paradigm consisted of overt (execution) tasks that, although fine for determining the suitability of a four-choice BCI, are impractical for people with motor disabilities.

One drawback of using the proposed scheme is that it does not detect neuronal firing directly but instead detects the change in blood flow that occurs as a result of neuronal firing; hence the inherent delay of approximately 2 s.[26,64,65] This haemodynamic delay in functional NIR spectroscopy response will not lead to high information transfer rates as compared with EEG-based BCI, even if four classes are considered. This might present a problem for real-time control of external devices using the scheme, though for decoding of applications, it does not matter much.

Regarding MA and MC tasks, the effects of habituation[66] and the differences between high- and low-skilled arithmetic task performers[67] were not considered in this study. Both factors might contribute to a low haemodynamic response over time. Furthermore, the MC task did not elicit strong signals, since it did not put a high cognitive load on the subjects. The MC task is therefore less suitable for BCI purposes compared with the other three tasks used in this study. This is also evident from the lower decoding percentage of option D which was associated with MC tasks.

Although dividing the experiment into different sessions and then recombining, the so-called session-to-session transfer, is common in BCI,[68,69] the practicality of the results is decreased because it is not feasible for real-time and online analysis.

A limitation of the proposed system is that it should be "synchronous" in the sense that the brain signal should be detected during the decision-making period and therefore will not work if the subject does not perform any of the recommend tasks during the response period.

One final factor of note is the healthy status of all of the subjects who participated in this study. Haemodynamic responses can differ in cases of people with LIS, ALS or other congenital or post-injury motor disabilities that usually result in relatively low classification accuracies.[10] It has been shown that classification accuracies can be increased using simultaneous EEG and fNIRS measurement to extract features.[54,70]

Conclusions

This study demonstrated the feasibility of a functional NIR spectroscopy-based four-class brain–computer interface by decoding answers to four-choice questions. The functional NIR spectroscopy signals arising from RMI, LMI, MA and MC were acquired in a "synchronous" way from the primary motor and prefrontal cortices, respectively. Using the SM and SS obtained during a 2~7 s segment from the 10 s task period, the four cognitive tasks were classified to an average accuracy of 73.3%.

Acknowledgements

This work was supported by the National Research Foundation of Korea under the Ministry of Science, ICT and Future Planning, Republic of Korea (grant no. NRF-2014-R1A2A1A10049727).

References

1. B. Sorger, B. Dahmen, J. Reithler, O. Gosseries, A. Maudoux, S. Laureys and R. Goebel, "Another kind of 'BOLD response': answering multiple-choice questions via online decoded single-trial brain signals", *Prog. Brain Res.* **177,** 275 (2009). doi: http://dx.doi.org/10.1016/S0079-6123(09)17719-1
2. J.R. Wolpaw, N. Birbaumer, D.J. McFarland, G. Pfurtscheller and T.M. Vaughan, "Brain–computer interfaces for communication and control", *Clin. Neurophysiol.* **113,** 767 (2002). doi: http://dx.doi.org/10.1016/S1388-2457(02)00057-3
3. B.A. Philip, N. Rao and J.P. Donoghue, "Simultaneous reconstruction of continuous hand movements from primary motor and posterior parietal cortex", *Exp. Brain Res.* **225,** 361 (2013). doi: http://dx.doi.org/10.1007/s00221-012-3377-0
4. M. Salvaris and F. Sepulveda, "Classification effects of real and imaginary movement selective attention tasks on a P300-based brain–computer interface", *J. Neural Eng.* **7,** 056004 (2010). doi: http://dx.doi.org/10.1088/1741-2560/7/5/056004
5. K. Choi, "Electroencephalography (EEG)-based neurofeedback training for brain–computer interface (BCI)", *Exp. Brain Res.* **231,** 351 (2013). doi: http://dx.doi.org/10.1007/s00221-013-3699-6
6. C. Enzinger, S. Ropele, F. Fazekas, M. Loitfelder, F. Gorani, T. Seifert, G. Reiter, C. Neuper, G. Pfurtscheller and G. Müller-Putz, "Brain motor system function in a patient with complete spinal cord injury following extensive brain–computer interface training", *Exp. Brain Res.* **190,** 215 (2008). doi: http://dx.doi.org/10.1007/s00221-008-1465-y
7. S.M. Coyle, T.E. Ward TE, C.M. Markham and G. McDarby (2004), "On the suitability of near-infrared (NIR) systems for next generation brain–computer interfaces", *Physiol. Meas.* **25,** 815 (2004). doi: http://dx.doi.org/10.1088/0967-3334/25/4/003
8. S.M. Coyle, T.E. Ward and C.M. Markham, "Brain–computer interface using a simplified functional near-infrared spectroscopy system", *J. Neural Eng.* **4,** 219 (2007). doi: http://dx.doi.org/10.1088/1741-2560/4/3/007
9. R. Sitaram, H. Zhang, C. Guan, M. Thulasidas, Y. Hoshi, A. Ishikawa, K. Shimizu and N. Birbaumer, "Temporal classification of multichannel near-infrared spectroscopy signals of motor imagery for developing a brain–computer interface", *NeuroImage* **34,** 1416 (2007). doi: http://dx.doi.org/10.1016/j.neuroimage.2006.11.005
10. M. Naito, Y. Michioka, K. Ozawa, Y. Ito, M. Kiguchi and T. Kanazaw, "A communication means for totally locked-in ALS patients based on changes in cerebral blood volume measured with near-infrared light", *IEICE Trans. Inform. Syst.* **90,** 1028 (2007). doi: http://dx.doi.org/10.1093/ietisy/e90-d.7.1028
11. X.-S. Hu, K.-S. Hong and S.S. Ge, "fNIRS-based online deception decoding", *J. Neural Eng.* **9,** 026012 (2012). doi: http://dx.doi.org/10.1088/1741-2560/9/2/026012
12. N. Naseer and K.-S. Hong, "Classification of functional near-infrared spectroscopy signals corresponding to the right- and left-wrist motor imagery for development of a brain–computer interface", *Neurosci. Lett.* **553**, 84 (2013). doi: http://dx.doi.org/10.1016/j.neulet.2013.08.021
13. N. Naseer, M.J. Hong and K.-S. Hong, "Online binary decision decoding using functional near-infrared spectroscopy for the development of brain computer interface", *Exp. Brain Res.* **232,** 555 (2014). doi: http://dx.doi.org/10.1007/s00221-013-3764-1
14. F.F. Jobsis, "Noninvasive, infrared monitoring of cerebral and myocardial oxygen sufficiency and circulatory parameters", *Science* **198**, 1264 (1977). doi: http://dx.doi.org/10.1126/science.929199
15. X.-S. Hu, K.-S. Hong, S.S. Ge and M.-Y. Jeong, "Kalman estimator- and general linear model-based on-line brain activation mapping by near-infrared spectroscopy", *Biomed. Eng. Online* **9,** 82 (2010). doi: http://dx.doi.org/10.1186/1475-925X-9-82
16. X.-S. Hu, K.-S. Hong and S.S. Ge, "Recognition of stimulus-evoked neuronal optical response by

identifying chaos levels of near-infrared spectroscopy time series", *Neurosci. Lett.* **504,** 115 (2011). doi: http://dx.doi.org/10.1016/j.neulet.2011.09.011

17. M. Aqil, K.-S. Hong, M.-Y. Jeong and S.S. Ge, "Cortical brain imaging by adaptive filtering of NIRS signals", *Neurosci. Lett.* **514,** 35 (2012). doi: http://dx.doi.org/10.1016/j.neulet.2012.02.048

18. M. Aqil, K.-S. Hong, M.-Y. Jeong and S.S. Ge, "Detection of event-related hemodynamic response to neuro-activation by dynamic modeling of brain activity", *NeuroImage* **63,** 553 (2012). doi: http://dx.doi.org/10.1016/j.neuroimage.2012.07.006

19. S. Cutini, S.B. Moro and S. Bisconti, "Functional near infrared optical imaging in cognitive neuroscience: an introductory review", *J. Near Infrared Spectrosc.* **20,** 75 (2012). doi: http://dx.doi.org/10.1255/jnirs.969

20. L.H. Ernst, S. Schneider, A.C. Ehlis, A.J. Fallgatter, "Functional near infrared spectroscopy in psychiatry: a critical review", *J. Near Infrared Spectrosc.* **20,** 93 (2012). doi: http://dx.doi.org/10.1255/jnirs.970

21. M. Ferrari, K.H. Norris and M.G. Sowa, "Medical near infrared spectroscopy 35 years after the discovery", *J. Near Infrared Spectrosc.* **20,** vii (2012).

22. M. Ferrari and V. Quaresima, "Near infrared brain and muscle oximetry: from the discovery to current applications", *J. Near Infrared Spectrosc.* **20,** 1 (2012). doi: http://dx.doi.org/10.1255/jnirs.973

23. M.A. Kamran and K.-S. Hong, "Linear parameter-varying model and adaptive filtering technique for detecting neuronal activities: an fNIRS study", *J. Neural Eng.* **10,** 056002 (2013). doi: http://dx.doi.org/10.1088/1741-2560/10/5/056002

24. S. Wijeakumar, U. Shahani, W.A. Simpson and D.L. McCulloch, "Haemodynamic responses to radial motion in the visual cortex", *J. Near Infrared Spectrosc.* **21,** 231 (2013). doi: http://dx.doi.org/10.1255/jnirs.1066

25. R. Bhutta, K.-S. Hong, B.-M. Kim, M.J. Hong, Y.-H. Kim and S.-H. Lee, "Note: three wavelength near-infrared spectroscopy system for compensating the light absorbance by water", *Rev. Sci. Instrum.* **85,** 026111 (2014). doi: http://dx.doi.org/10.1063/1.4865124

26. K.-S. Hong and H.-D. Nguyen, "State-space models of impulse hemodynamic responses over motor, somatosensory and visual cortices", *Biomed. Opt. Express* **5,** 1778 (2014). doi: http://dx.doi.org/10.1364/BOE.5.001778

27. B. Xu, Y. Fu, G. Shi, X. Yin, Z. Wang and H. Li, "Improving classification by feature discretization and optimization for fNIRS-based BCI", *J. Biomim. Biomater. Tissue Eng.* **19,** 1000119 (2014). doi: http://dx.doi.org//10.4172/1662-100X.1000119

28. G. Bauernfeind, R. Leeb, S.C. Wriessnegger and G. Pfurtscheller, "Development, set-up and first results for a one-channel near-infrared spectroscopy system", *Biomed. Tech.* **53,** 36 (2008). doi: http://dx.doi.org/10.1515/BMT.2008.005

29. S.D. Power, T.H. Falk and T. Chau, "Classification of prefrontal activity due to mental arithmetic and music imagery using hidden Markov models and frequency domain near-infrared spectroscopy", *J. Neural Eng.* **7,** 026002 (2010). doi: http://dx.doi.org/1088/1741-2560/7/2/026002

30. S.D Power, A. Khushki and T. Chau, "Towards a system-paced near-infrared spectroscopy brain–computer interface: differentiating prefrontal activity due to mental arithmetic and mental singing from the no-control state", *J. Neural Eng.* **8,** 066004 (2011). doi: http://dx.doi.org/10.1088/1741-2560/8/6/066004

31. S.D Power, A. Khushki and T. Chau, "Automatic single trial discrimination of mental arithmetic, mental singing and the no-control state from the prefrontal activity: towards a three-state NIRS-BCI", *BMC Res. Notes* **5,** 141 (2012). doi: http://dx.doi.org/10.1186/1756-0500-5-141

32. J. Li and L. Zhang, "Active training paradigm for motor imagery BCI", *Exp. Brain Res.* **219,** 245 (2012). doi: http://dx.doi.org/10.1007/s00221-012-3084-x

33. J. Yue, Z. Zhou, J. Jiang, Y. Liu and D. Hu, "Balancing a simulated inverted pendulum through motor imagery: an EEG-based real-time control paradigm", *Neurosci. Lett.* **524,** 95 (2010). doi: http://dx.doi.org/10.1016/j.neulet.2012.07.031

34. M. Stangl, G. Bauernfiend, J. Kurzmann, R. Scherer and C. Neuper, "A haemodynamic brain–computer interface based on real-time classification of near infrared spectroscopy signals during motor imagery and mental arithmetic", *J. Near Infrared Spectrosc.* **21,** 157 (2012). doi: http://dx.doi.org/10.1255/jnirs1048

35. S.C. Cramer, L. Lastra, M.G. Lacourse and M.J. Cohen, "Brain motor system function after chronic, complete spinal cord injury", *Brain* **128,** 294 (2005). doi: http://dx.doi.org/10.1093/brain/awh648

36. E. Lopez-Larraz, J.M. Antelis, L. Montesano, A. Gil-Agudo and J. Minguez, "Continuous decoding of motor attempt and motor imagery from EEG activity in spinal cord injury patients", Conference Proceedings, IEEE Engineering in Medicine and Biology Society, pp. 1789–1801 (2012).

37. J. Chan, S. Power and T. Chau, "Investigating the need for modelling temporal dependencies in a brain–computer interface with real-time feedback based on near infrared spectra", *J. Near Infrared Spectrosc.* **20,** 107 (2012). doi: http://dx.doi.org/10.1255/jnirs.971

38. G. Strangman, D.A. Boas and J.P. Sutton, "Non-invasive neuroimaging using near-infrared light", *Biol. Psychiatry* **52,** 679 (2002). doi: http://dx.doi.org/10.1016/S0006-3223(02)01550-0

39. S. Luu and T. Chau, "Decoding subjective preferences from single-trial near-infrared spectroscopy signals", *J. Neural Eng.* **6,** 016003 (2009). doi: http://dx.doi.org/10.1088/1741-2560/6/1/016003

40. N.J. Hill, E. Ricci, S. Haider, L.M. McCane, S. Heckman, J.R. Wolpaw and T.M. Vaughan, "A practical, intuitive brain–computer interface for communicating 'yes' or 'no' by listening", *J. Neural Eng.* **11,** 035003 (2014). doi: http://dx.doi.org/10.1088/1741-2560/11/3/035003

41. J.-H. Lim, H.-J. Hwang, S.-H. Han, K.-Y. Jung and C.-H. Im, "Classification of binary intentions for individuals with impaired oculomotor function: 'eyes-closed' SSVEP-based brain–computer interface (BCI)", *J. Neural Eng.* **10,** 026021 (2013). doi: http://dx.doi.org/10.1088/1741-2560/10/2/026021

42. Y. Hoshi, "Functional near-infrared spectroscopy: current status and future prospects", *J. Biomed. Opt.* **12,** 062106 (2007). doi: http://dx.doi.org/10.1117/1.2804911

43. D.T. Delpy, M. Cope, P. van der Zee, S. Arridge, S. Wray and J. Wyat, "Estimation of optical path length through tissue from direct time of flight measurement", *Phys. Med. Biol.* **33,** 1433 (1988). doi: http://dx.doi.org/10.1088/0031-9155/33/12/008

44. R.W. Homan, J. Herman and P. Purdy, "Cerebral location of international 10-20 system electrode placement", *Electroen. Clin. Neuro.* **66,** 376 (1987). doi: http://dx.doi.org/10.1016/0013-4694(87)90206-9

45. P.W. McCormick, M. Stewart, G. Lewis, M Dujovny and J.I. Ausman, "Intracerebral penetration of infrared light", *J. Neurosurg.* **76,** 315 (1992). doi: http://dx.doi.org/10.3171/jns.1992.76.2.0315

46. G. Gratton, C.R. Brumback, B.A. Gordon, M.A. Pearson, K.A. Low and M. Fabiani, "Effects of measurement method, wavelength and source-detector distance on the fast optical signal", *NeuroImage* **32,** 1576 (2006). doi: http://dx.doi.org/ 10.1016/j.neuroimage.2006.05.030

47. B.D. Frederick, L.D. Nickerson and Y. Tong, "Physiological denoising of BOLD fMRI data using regressor interpolation at progressive time delays (RIPTiDe) processing of concurrent fMRI and near-infrared spectroscopy (NIRS)", *NeuroImage* **60,** 1913 (2012). doi: http://dx.doi.org/10.1016/j.neuroimage.2012.01.140

48. R. Beisteiner, P. Hollinger, G. Lindinger, W. Lang and A. Berthoz, "Mental representations of movements: brain potentials associated with imagination of hand movements", *Electroencephalogr. Clin. Neurophysiol.* **96,** 183 (1995). doi: http://dx.doi.org/10.1016/0168-5597(94)00226-5

49. C.A. Porro, M.P. Francescato, V. Cettolo, M.E. Diamond, P. Baraldi, C. Zuiani, M Bazzocchi and P.E. di Prampero, "Primary motor and sensory cortex activation during motor performance and motor imagery: a functional magnetic resonance imaging study", *J. Neurosci.* **16,** 7688 (1996).

50. J.C. Ye, S. Tak, K.E. Jang, J. Jung and J. Jang, "NIRS-SPM: statistical parametric mapping for near-infrared spectroscopy", *NeuroImage* **44,** 428 (2009). doi: http://dx.doi.org/10.1016/j.neuroimage.2008.08.036

51. H. Santosa, M.J. Hong, S.-P. Kim and K.-S. Hong, "Noise reduction in functional near-infrared spectroscopy signals by independent component analysis", *Rev. Sci. Instrum.* **84,** 073106 (2013). doi: http://dx.doi.org/10.1063/1.4812785

52. M.A. Kamran and K.-S. Hong, "Reduction of physiological effects in fNIRS waveforms for efficient brain-state decoding," *Neurosci. Lett.* **580,** 130 (2014). doi: http://dx.doi.org/10.1016/j.neulet.2014.07.058

53. S. Fazli, J. Mehnert, J. Steinbrink, G. Curio, A. Villringer, K.R Muller and B. Blankertz, "Enhanced performance by a hybrid NIRS-EEG brain computer interface", *NeuroImage* **59,** 519 (2012). doi: http://dx.doi.org/10.1016/j.neuroimage.2011.07.084

54. M.J. Khan, M.J. Hong and K.-S. Hong, "Decoding of four movement directions using hybrid NIRS-EEG brain–computer interface", *Front. Hum. Neurosci.* **8**, 00244 (2014). doi: http://dx.doi.org/10.3389/fnhum.2014.00244

55. K.-S. Hong, N. Naseer and Y.-H. Kim, "Classification of prefrontal and motor cortex signals for three-class fNIRS-BCI", *Neurosci. Lett.* **587,** 87 (2015). doi: http://dx.doi.org/http://dx.doi.org/10.1016/j.neulet.2014.12.029

56. N. Naseer and K.-S. Hong, "fNIRS-based brain–computer interfaces: a review", *Front. Hum Neurosci.* **9,** 3 (2015). doi: http://dx.doi.org/10.3389/fnhum.2015.00003

57. F. Lotte, M. Congedo, A. Lecuyer, F. Lamarche and B. Arnaldi, "A review of classification algorithms for EEG-based brain–computer interfaces", *J. Neural Eng.* **4** (2007). doi: http://dx.doi.org/10.1088/1741-2560/4/2/R01

58. T. Li, S. Zhu and M. Ogihara, "Using discriminant analysis for multi-class classification: an experimental investigation", *Knowl. Inf. Syst.* **10,** 453 (2006). doi: http://dx.doi.org/10.1007/s10115-006-0013-y

59. T. Yarkoni and T.S. Braver, "Cognitive neuroscience approaches to individual differences in working memory and executive control: conceptual and methodological issues", in *Handbook of Individual Differences in Cognition: Attention, Memory and Executive Control*, Ed by A. Gruszka, G. Matthews and B. Szymuyra. Springer, New York, p. 87 (2010).

60. X.-S. Hu, K.-S. Hong and S.S. Ge, "Reduction of trial-to-trial variations in functional near-infrared spectroscopy signals by accounting for resting-state functional connectivity", *J. Biomed. Opt.* **18,** 017003 (2013) doi: http://dx.doi.org/10.1117/1.JBO.18.1.017003

61. L. Holper, N. Kobashi, D. Kiper, F. Scholkmann, M. Wolf and K. Eng, "Trial-to-trial variability differentiates motor imagery during observation between low versus high responders: a functional near-infrared spectroscopy study", *Behav. Brain Res.* **229,** 29 (2012). doi: http://dx.doi.org/10.1016/j.bbr.2011.12.038

62. H. Santosa, M.J. Hong and K.-S. Hong, "Laterization of music processing with noise in the auditory cortex: an fNIRS study", *Front. Behav. Neurosci.* **8,** 418 (2014). doi: http://dx.doi.org/ http://dx.doi.org/ 10.3389/fnbeh.2014.00418

63. J. Shin and J. Jeong, "Multiclass classification of hemodynamic responses for performance improvement of functional near-infrared spectroscopy-based brain–computer interface", *J. Biomed. Opt.* **19,** 067009 (2014). doi: http://dx.doi.org/10.1117/1.JBO.19.6.067009

64. F.M. Miezin, L. Maccotta, .M. Ollinger, S.E. Petersen and R.L. Buckner, "Characterizing the hemodynamic response: effects of presentation rate, sampling procedure and the possibility of ordering brain activity based on relative timing", *NeuroImage* **11,** 735 (2000). doi: http://dx.doi.org/10.1006/nimg.2000.0568

65. G. Jasdzewski, G. Strangman, J. Warner, K.K. Kwong, R.A. Poldrack and D.A. Boas, "Differences in the hemodynmics reponse to event-related motor and visual paradigms as measured by near-infrared spectroscopy", *NeuroImage* **20,** 279 (2003). doi: http://dx.doi.org/10.1016/S1053-8119(03)00311-2

66. A. Szabo and L. Gauvin, "Reactivity to written mental arithmetic: effects of exercise lay-off and habituation", *Physiol. Behav.* **51,** 501 (1992). doi: http://dx.doi.org/10.1016/0031-9384(92)90171-W

67. M.I. Nunez-Pena and M. Suarez-Pellicioni, "Processing false solutions in additions: differences between high- and lower-skilled arithmetic problem-solvers", *Exp. Brain Res.* **218,** 655 (2012). doi: http://dx.doi.org/10.1007/s00221-012-3058-z

68. S. Fazli, M. Danoczy, J. Schelldorfer and K.R Muller, "l1-penalized linear mixed-effects models for BCI", in *Artificial Neural Networks and Machine Learning—ICANN 2011*, Ed by T. Honkela, W. Duch, M. Girolami and S. Kaski. Springer, Berlin, p. 26 (2011).

69. S. Fazli, F. Popescu, M. Danoczy, B. Blankertz, K.R. Muller and C. Grozea, "Subject-independent mental state classification in single trials", *Neural Networks* **22,** 1305 (2009). doi: http://dx.doi.org/10.1016/j.neunet.2009.06.003

70. M. Biallas, I. Trajkovic, D. Haensse, V. Marcar and M. Wolf, "Reproducibility and sensitivity of detecting brain activity by simultaneous electroencephalography and near-infrared spectroscopy", *Exp. Brain Res.* **222,** 255 (2013). doi: http://dx.doi.org/10.1007/s00221-012-3213-6